Journal of Applied Automation Technologies

Research Paper

Dynamic Sensor Fusion Algorithm Enhances SLAM Performance in Unknown Environments

Olaf Tadeusz Truskolaski[1], Barbara Grabowska[1] and Eugeniusz Stępień[1, *]

[1] Faculty of Automation and Mechatronics, University of Applied Sciences in Kalisz, Kalisz, 62-800, Poland
*Corresponding author: eugeniusz.s@wsz-kalisz.pl

Abstract. Robots operating in unfamiliar and unstructured surroundings can now perform better with Simultaneous Localisation and Mapping (SLAM) thanks to dynamic sensor fusion. By building a system that can adaptively combine the data streams of vision, inertia, and LiDAR through online reliability analysis and dynamic weight adjustment, this work aims to address the long-standing problems of robust real-time localisation and mapping (SLAM). To increase the system's resilience to sensor dropouts, environmental variations, and abrupt scene changes, continuously evaluate each sensor's degree of trust in the suggested system and dynamically modify its weights while it is in use. The approach has been proven to reduce root-mean-square trajectory error by more than 30% when compared to static fusion and single-modality baselines, and it has been confirmed in both structured indoor and challenging outdoor experiments. The findings of the robustness test demonstrate that the system can still map and locate the robot normally after 40 frames following a sensor failure. According to ablation research, both are required for online reliability estimation and adaptive fusion to operate consistently. The aforementioned findings indicate that the technique has been refined to lower the mean latency to less than 40 milliseconds for designing real-time processing. In general, this approach has raised the bar for SLAM's resilience, precision, and effectiveness in domains lacking prior information and environmental consistency presumptions.

Keywords: *Sensor Fusion, SLAM, Autonomous Robotics, Real-Time Processing, Robust Mapping*

Received on 03 December 2024, Accepted on 05 May 2025, Published on 13 May 2025

Introduction

Many high-level accomplishments in self-navigating ground vehicles, aerial drones, and other complex-environment industrial and service robots have been made possible by the application of Simultaneous Localisation and Mapping (SLAM) in the creation of autonomous robotics [1]. In order to enable safe and adaptable operation of robots in real surroundings, SLAM aims to have a system jointly develop a model of the environment and its own location in the absence of a pre-built map. Over the past few decades, this subject has garnered substantial research [2]. For high-demand applications, such as extended-range exploration, infrastructure inspection, dynamic logistics, etc., robust localisation and trustworthy mapping are currently required; manual operation or global reference systems cannot be used [3]. Many researchers have integrated the benefits of multiple sensors, including cameras, IMUs, and LiDAR, to create high-precision, stable, multi-modal systems, even though the previous work only employed one type of sensor [4]. Robots can avoid issues like moving objects, a lack of roughness in the surroundings, and sensor noise by combining these numerous sensors in a variety of settings [5]. However, sensor bias, perceptual aliasing, and abrupt changes in scene structure make typical SLAM pipelines vulnerable to failure in open or unfamiliar situations [6].

Recent studies on multi-sensor fusion have been conducted in light of the aforementioned issues. Integrate a variety of sensory data to enhance position and orientation accuracy and solve issues that a single sensor model may have, such as drift, range ambiguity, scale inconsistencies, etc. [7]. Additionally, dynamically fused sensor fusion techniques have demonstrated good performance in handling non-stationary settings and automatically modifying the weightings of different sensors to adapt their influence on the fly [8]. In order to identify outliers and quantify measurement uncertainty, state-of-the-art techniques include statistical models, confidence-weighted filtering, or learning-based procedures. They can also consistently recover following a sensor failure [9]. Even though the aforementioned are useful, many of the existing approaches rely on static fusion strategies, heuristic parameter tweaks, or inadequate adaptation to new contexts, making them unsuitable for responding to large or abrupt changes in the environment [10].

This study presents a dynamic, context-aware sensor fusion technique for new-generation SLAM applications in light of current technological shortcomings and the need to employ autonomous systems in unique and unpredictable situations. A multi-sensor fusion structure has been used to improve the accuracy of the map and strengthen the robustness of SLAM in order to adapt to various changes in the working environment. In light of the necessity for self-tuning and fault-tolerant characteristics in the fusion process, this study attempts to address the existing issues with SLAM systems in uncontrolled environments, hence offering new paths for autonomous exploration and operation in real-world scenarios.

Related Work

Progress and Challenges in SLAM for Unknown and Unstructured Environments

The topic of autonomous mapping without previous information in many situations has improved with the development of Simultaneous Localisation and Mapping (SLAM), which has progressed from early probabilistic filtering models to scalable systems based on factor graphs and pose graph optimisation [11]. SLAM systems are currently not very stable in unfamiliar or unstructured contexts, though; problems including perceptual aliasing, dynamic scene features, and environmental ambiguity frequently result in inconsistent mapping or localisation failure [12]. Dealing with moving objects, maintaining trajectory accuracy in low-feature or textureless areas, and recovering from localisation loss in unpredictable places are recurring issues [13].

Although many conventional SLAM algorithms still make simplifying assumptions or employ fixed thresholds that limit their practical applicability, researchers have recently worked to increase the robustness of SLAM systems in non-stationery and feature-scarce situations [14]. Even while some modern methods that combine LiDAR and vision-inertial data have done rather well in challenging conditions, they still have issues including uneven sensor distribution, sensitivity to changes in light, and relatively substantial mapping errors in dense areas [15].

Advances and Limitations in Multi-Sensor Fusion

Currently, multiple-sensor fusion is needed to integrate complementary data from vision, IMU, and LiDAR in order to guarantee the stability and accuracy of SLAM initialisation and trajectory tracking under uncertainty [16]. Probability-based fusion techniques, like factor graph optimisation and Bayesian filtering, have been applied to increase data association reliability and robustness to partial sensor failures [17]. The majority of existing multi-sensor SLAM systems are not suitable for situations with sudden or unpredictable changes in operation because they either use empirical, manually calibrated weights or have preset fusion parameters [18].

As contemporary sensor systems have evolved, a variety of types have progressively emerged, and issues including disparate collection schedules, uneven measurement rates, and sensor drift are now rather significant [19]. These fusion frameworks' calibrations, inadequate temporal synchronisation, and restricted real-time processing capabilities limit their practical adaptability and scalability, particularly when dealing with abrupt sensor changes or environmental disruptions [20].

Shortcomings of Current Dynamic Fusion Approaches and Research Gap

Even while adaptive fusion has advanced, many dynamic approaches still rely on heuristic outlier rejection procedures or preset uncertainty models, which makes them vulnerable to real-world changes [21]. Algorithms are not really context-aware since they may perform poorly or become unstable in situations including sudden sensor deterioration, abrupt changes in the environment, or malevolent adversary interventions [22]. Though they may overfit to the training environment and fail to explain actions in safety-critical applications, learning-based dynamic fusion techniques are similarly promising but come with computational costs and generalisation hazards [23]. One major unresolved issue in SLAM research is autonomous and dependable performance in unpredictable or dynamic contexts that is nonetheless effective and comprehensible [24].

Consequently, creating SLAM frameworks that are both context-aware and self-adaptive remains a significant research challenge; that is, they must be able to dynamically react to both gradual and abrupt changes in the operating environment, intelligently modify sensor weights, and robustly filter out outlier information. For usage in the state-of-the-art of robot research and application, a technique for continuous, dependable SLAM in extremely wide or unconstrained environments has been devised to solve this shortcoming [25].

Theoretical Framework

System Framework Overview

To accomplish robust, real-time localisation and mapping in unfamiliar and challenging situations, a modular and hierarchical architecture has been developed for the suggested dynamic sensor fusion SLAM system. LiDAR, inertial, and optical sensors are the three types of data sources used at the bottom of the system to create a SLAM back-end. In order to get continuous motion priors in the event of visual obstruction or scan sparsity, the core data flow starts with a synchronised acquisition of high-rate inertial measurements. Hybrid geometric and photometric tracking is used because inertial inputs are time-synchronized with visual observations from a multi-camera array, such as a stereo or RGB-D system.

Planar patches, edge points, and other conspicuous geometric features that are resilient to both texture-poor and intensely lighted circumstances are retrieved for dependable registration after the raw LiDAR scans are processed independently using a solid feature extraction method. To increase the global map's consistency over a long baseline and lessen visual ambiguity, add a set of sparse restrictions from each LiDAR scan to the joint optimisation layer.

During the bundle adjustment of multi-sensory constraints, a global fusion engine acts as the system's computational hub and dynamically modifies the degree of confidence or impact of each sensor stream. The signal-to-noise ratio, field-of-view occlusion, and scene-dependent deterioration effects of all sensory inputs are calculated using an online sensor reliability estimator. All multi-rate sensor data will be combined into a tightly-coupled factor graph model using real-time calibration and temporal synchronisation procedures.

The corresponding modules for sensor-specific preprocessing, data association, spatial-temporal alignment, and outlier rejection are all rather straightforward, as seen in Figure 1. The modules are linked to the higher optimisation module, and the global optimum of the platform's trajectory and the environment map's structure are found using probabilistic inference and direct optimisation. Because the system is plug-and-playing adaptable, future additions of new sensor types can satisfy real-time needs for unstructured and unfamiliar settings.

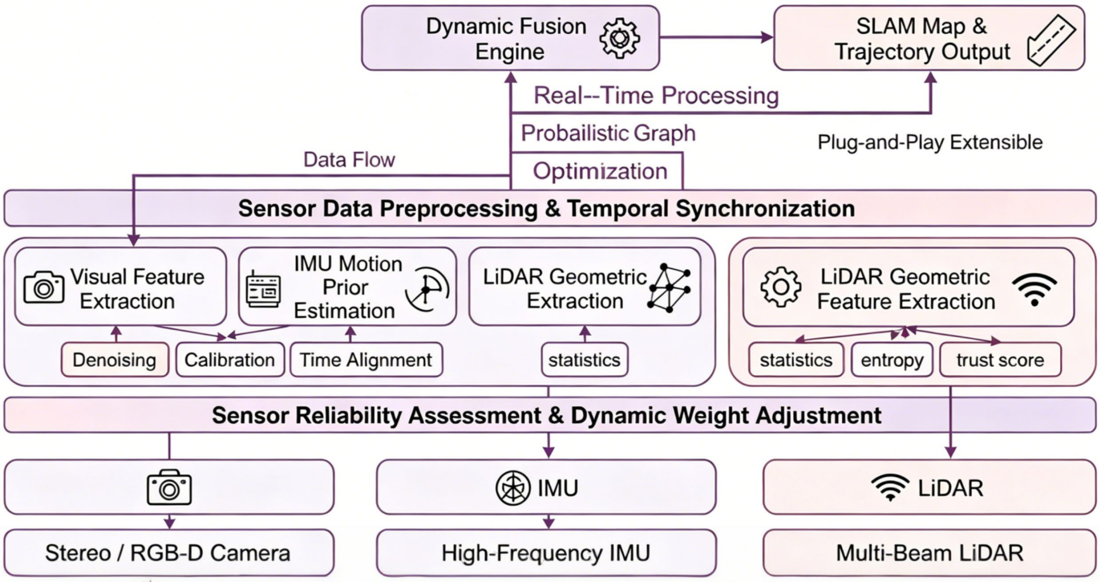

Figure 1. System Architecture of Dynamic Sensor Fusion SLAM: Synchronized Multi-Sensor Streams, Dynamic Fusion Engine, and Centralized Optimization Block.

Dynamic Sensor Fusion Algorithm

Our SLAM framework's dynamic fusion algorithm is based on an accurate and flexible integration technique for a variety of sensors in the face of real-world uncertainty. The system's fusion engine continuously gathers data from all sensor streams, including vision, inertia, and LiDAR, and dynamically modifies the weights of this data based on scene conditions and signal strength.

In order to minimise noise in inertial data, detect reprojection errors in visual features, and confirm geometric consistency of LiDAR points, the raw sensor data will be debiased and filtered at the time of acquisition. The multi-sensor graph propagates only well-conditioned measurements. As a result, misleading local minima in the downstream optimisation are prevented and the spread of correlated noise is decreased.

The core of the dynamic fusion is an online sensor trust evaluator, which quantifies each sensor's instantaneous reliability using both statistical and information-theoretic metrics derived from their recent performance history. The adaptive weight w_i^t assigned to each sensor i at time t is computed as a normalized function of predicted measurement covariance, spatial consistency, and real-time entropy of observations. The fusion update rule for the robot's state vector $\mathbf{x}_t$ thus considers the full weighted multi-sensor information, in contrast to conventional static models.

$$\mathbf{x}_t^* = \arg\min_{\mathbf{x}_t} \left\{ \sum_{i=1}^{N} w_i^t \left\| \mathbf{z}_{i,t} - h_i(\mathbf{x}_t) \right\|_{\boldsymbol{\Sigma}_{i,t}^{-1}}^2 \right\} \quad \text{Eq.(1)}$$

Here, $\mathbf{z}_{i,t}$ denotes the observation from sensor i at time t, h_i is the corresponding observation model, $\boldsymbol{\Sigma}_{i,t}$ the covariance, and w_i^t they learned reliability.

Sensor weights are updated recursively based on a predictive reliability score, which incorporates the last K time steps and penalizes abrupt deviations via a temporal smoothing prior:

$$w_i^t = \frac{\exp\left(-\alpha S_{i,t}\right)}{\sum_j \exp\left(-\alpha S_{j,t}\right)} \quad \text{Eq.(2)}$$

where $S_{i,t}$ is a composite score reflecting the Mahalanobis innovation distance, entropy variation, and transient failure flags, and α is a sharpening parameter ensuring rapid downweighting of unreliable streams.

For handling outliers and sudden sensor failures, we introduce a two-stage rejection mechanism. First, a statistical innovation test detects anomalous updates by thresholding the normalized residuals:

$$\text{Reject: } \left\|\mathbf{z}_{i,t} - h_i(\mathbf{x}_t)\right\| > \gamma\left(\operatorname{tr}(\boldsymbol{\Sigma}_{i,t})\right)^{1/2} \quad \text{Eq.(3)}$$

where γ is adaptively set based on the ambient environmental variability.

Secondly, at the graph level, loop-closure and global consistency checks utilize a robust loss function from the generalized M-estimator class, markedly suppressing the effect of isolated or persistent outliers within the multi-sensor trajectory reconstruction:

$$\rho(\xi) = \frac{\xi^2}{1+\lambda|\xi|}, \xi \in \{ \text{ All residuals in the fused factor graph } \} \quad \text{Eq.(4)}$$

In addition to these measures, the algorithm dynamically estimates the uncertainty envelope for each state via higher-order unscented transforms, propagating both sensor noise and process uncertainty through nonlinear dynamics:

$$\mathbf{P}_t = \sum_{m=1}^{2L+1} \omega_m [f(\mathbf{x}_{t-1}^m, \mathbf{u}_{t-1}) - \hat{\mathbf{x}}_t][f(\mathbf{x}_{t-1}^m, \mathbf{u}_{t-1}) - \hat{\mathbf{x}}_t]^\top \quad \text{Eq.(5)}$$

where f is the nonlinear prediction model, $\mathbf{u}_{t-1}$ the control input, ω_m weights, and L the system state dimension.

The fusion process actively leverages cross-modality correlation by quantifying mutual information between sensors at each step. If the mutual information of a given sensor falls below a dynamic threshold, its relative weight is automatically decreased in the fusion scheme:

$$I(\mathbf{z}_{i,t}; \mathbf{z}_{j,t}) < \tau \Longrightarrow w_i^t \downarrow \quad \text{Eq.(6)}$$

This tightly-coupled and context-aware fusion mechanism enables the SLAM system to sustain high-precision mapping and localization even as underlying sensor conditions, scene statistics, or operational complexity evolve unpredictably.

Adaptivity to Unknown Environments

A flexible mode that can adapt to changes in this state and automatically alter algorithm behaviour in real time is necessary given the current unpredictable operational environment. To allow the fusion engine to systematically modify the operation of sensors, noise models, and failure response mechanisms in response to changes in the environment and sensor health, a Layered Adaptivity Module has been introduced to the proposed framework.

Environmental awareness is achieved by constructing a compact set of environmental descriptors at each time step. These descriptors encapsulate feature density, motion saliency, illumination variance, and geometric structural cues extracted from sensor data streams. The system maintains a real-time environmental complexity score, C_t, derived by aggregating spatiotemporal statistics and recurrence indicators over a sliding window. This metric is fundamental to modulating the system's estimation confidence and fusion aggressiveness. The environment-aware adjustment of fusion fidelity is formalized as:

$$\beta_t = \frac{1}{1+\exp\left(-\kappa(C_t - C_0)\right)} \quad \text{Eq.(7)}$$

where β_t acts as a non-linear gating factor for measurement covariance inflation, C_0 is the nominal complexity baseline, and κ controls the sharpness of adaptivity. When C_t rises, for example due to rapidly changing appearance or dense dynamic obstacles, the system inflates measurement noise covariances, thereby automatically reducing the influence of less reliable sensor updates in the optimization.

In parallel, the SLAM engine continuously monitors each sensor's functional status by integrating cross-modal consistency checks and internal quality scores. Sensor health is scored through a recurrent evaluation framework, producing a vector $\mathbf{h}_t$ that captures recent failure modes, dropout rates, and drift trends. This vector modulates the sensor trust parameters and triggers redundancy logic:

$$\mathbf{h}_t = \lambda_1 \operatorname{std}(\mathbf{z}_{i,t-T:t}) + \lambda_2 \Delta r_{i,t} + \lambda_3 f_{\text{drop},i} \quad \text{Eq.(8)}$$

where $\mathrm{std}(\mathbf{z}_{i,t-T:t})$ is the rolling standard deviation of the sensor's measurements over a temporal window $T, \Delta r_{i,t}$ represents the rate of innovation change, $f_{\text{drop},i}$ is the dropout count, and λ_k are sensor-specific weighting coefficients.

The system's fault-tolerant mode will be triggered if a protracted decline in sensor quality or hardware breakdown is detected. This procedure will enhance the uncertainty of the compromised measurements and automatically reroute fusion priorities to the more dependable modalities. The method will transition to a conservative state-propagation mode if a missing sensor is necessary for geometric observability, and it will continue to do so until the sensor health improves.

Together, environmental sensitivity and autonomous sensor health management preserve the SLAM system's accuracy and stability in the face of abrupt environmental changes, significant obstruction, or partial sensor failure. Building an adaptive, robust autonomous system that can operate regularly in unfamiliar circumstances is therefore essential.

Experimental Procedures

Experimental Platform and Scenarios

A tactically positioned high-frequency inertial measurement unit (IMU), a stereo vision system with synchronised global shutter cameras, and a cutting-edge multi-beam LiDAR are all features of the experimental platform. Every module should be fixed to lessen the impact of outside disturbances, and calibration should be done continuously on uneven terrain and during high-dynamic manoeuvres. With an end-to-end pipeline response time of less than 50 milliseconds, the onboard computational stack is a real-time Linux distribution with a Jetson Xavier AGX for high-level parallel perception and adaptive fusion.

Experiments will be carried out both outside and in a challenging indoor environment. A sizable industrial area with shiny surfaces, high illumination gradients, both stationary and moving objects, and a variety of occlusion and appearance aliasing scenarios is used to construct up indoor trajectories. Rough terrain, grass and gravel, shifting sunshine, shadow passages, and dynamic occlusions from moving targets and ambient elements like fog are all characteristics of outdoor missions. To find module failure sites, stress tests are conducted on each sensor independently before integrating them all. Every deployment is continually validated using closed-loop calibration targets, and sub-millisecond time synchronisation and high-precision spatial calibration are always maintained. figure 2 depicts the sensor's topology, fields of view, and rationale for layout; for simplicity, this picture will be cited frequently in the ensuing analysis.

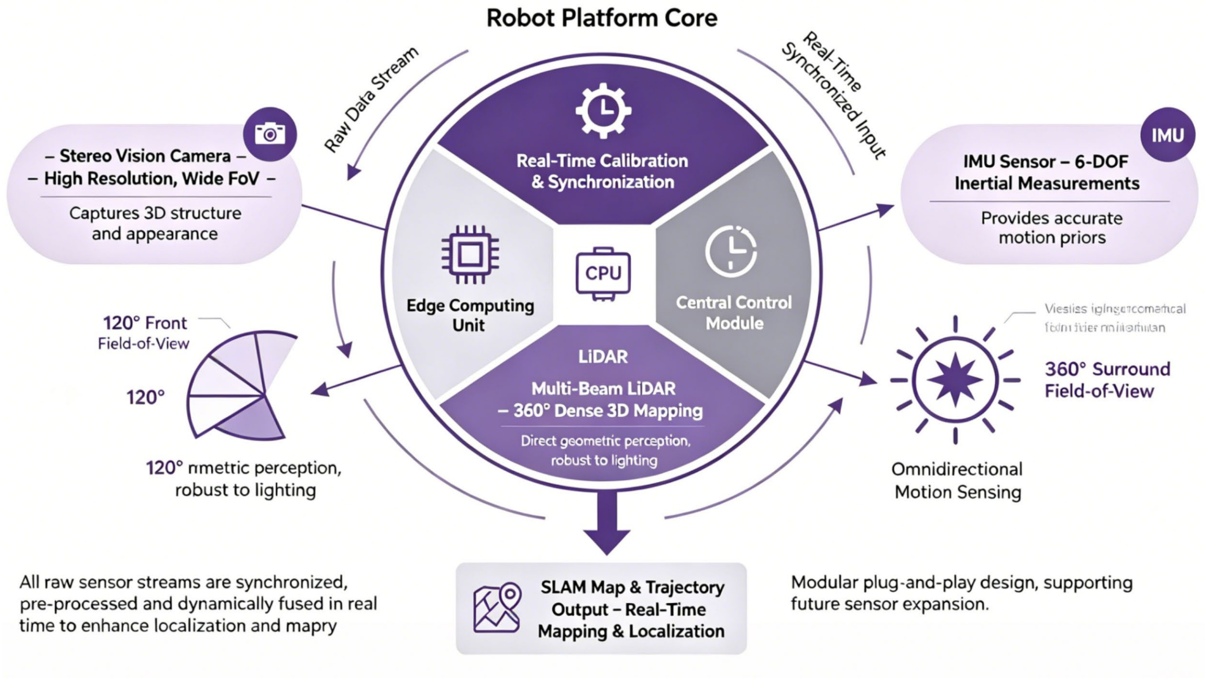

Figure 2. Experimental Sensor Arrangement and Platform Architecture for SLAM Validation.

Evaluation Protocols and Metrics

Motion-capture beacons are used to create an indoor reference, while RTK-corrected GNSS and survey markers are used for outdoor location. All experimental trajectories are referenced to centimeter-level ground-truth. Conduct the experiment in a variety of settings, at varied speeds, and with numerous sets of active sensors. Trajectory error, estimate uncertainty, processing speed, and robustness to simulated sensor failure are all included in performance quantification.

The trajectory error is measured using a temporally synchronized root-mean-square error formulation, explicitly modeling spatial and temporal drift accumulation:

$$\mathrm{RMSE} = \left(\frac{1}{T}\int_0^T \|p_{\mathrm{est}}(t) - p_{\mathrm{ref}}(t)\|^2 \, \mathrm{d}t\right)^{1/2} \qquad \text{Eq.(9)}$$

where $p_{\text{est}}(t)$ and $p_{\text{ref}}(t)$ represent estimated and ground-truth positions along the trajectory.

To gauge the information gain and calibration stability with respect to baseline methods, the Information Consistency Index is computed by comparing log-determinants of covariance matrices for fused versus single-modality solutions at synchronized keyframes:

$$\mathrm{ICI} = \frac{1}{K}\sum_{k=1}^{K} \frac{|\log \det P_{\mathrm{fusion}}(k) - \log \det P_{\mathrm{baseline}}(k)|}{\log \det P_{\mathrm{fusion}}(k)} \qquad \text{Eq.(10)}$$

where P_{fusion} and P_{baseline} are error covariances at instant k.

Frame processing performance and overload resilience are quantified using the aggregate throughput index as follows:

$$\mathrm{ATI} = \frac{1}{S}\sum_{s=1}^{S} \frac{f_s^{\mathrm{out}}}{f_s^{\mathrm{nom}} + \varphi(|\dot{\theta}_s| + |\ddot{\theta}_s|)} \qquad \text{Eq.(11)}$$

with f_s^{out} the output (processed) frequency, f_s^{nom} the nominal input frequency, and φ a penalty factor incorporating platform angular velocity and acceleration.

System resilience to unexpected sensor failures is quantified by fault tolerance, where recovery time and estimation quality after induced sensor outages are aggregated into a single metric:

$$\mathrm{FTS} = \frac{1}{N}\sum_{n=1}^{N} \Phi_n \left[1 - \exp\left(-\frac{\Delta t_n^{\mathrm{rec}}}{\tau}\right)\right] \quad \text{Eq.(12)}$$

In this equation, Φ_n marks the system's recovery status, $\Delta t_n^{\mathrm{rec}}$ is the recovery interval, and τ the characteristic robustness timescale.

Summary and Control Design

In order to verify the adaptability and computational stability of the SLAM system, all experimental procedures strive for reproducibility and establish high requirements for environmental complexity and dynamic scenarios. For statistical verification, the same path is traversed several times at different speeds, light levels, and sensor activation modes. To evaluate the lower-level fusion and adaptability mechanisms, create controlled sensor drop-out and recovery cycles.

Holistic performance evaluation is captured through an integrated metric constructed to weight trajectory accuracy, throughput, and multi-sensor consistency in a unified scale:

$$\mathrm{IPM} = \omega_1\left(1 - \frac{\mathrm{RMSE}}{\mathrm{RMSE}_0}\right) + \omega_2\frac{\mathrm{ATI}}{\mathrm{ATI}_0} + \omega_3\frac{\mathrm{ICI}}{\mathrm{ICI}_0} \quad \text{Eq.(13)}$$

where weights ω_1, ω_2, and ω_3 are scenario-dependent and reference values are set by baseline performance in ideal conditions.

For closed-loop trajectory validation, execution consistency is tracked by comparing planned and actual control command time series across all trials:

$$\mathrm{CCF} = \frac{1}{M}\sum_{m=1}^{M} \left|u_m^{\mathrm{plan}} - u_m^{\mathrm{act}}\right| \quad \text{Eq.(14)}$$

with u_m^{plan} and u_m^{act} representing expected and enacted platform inputs at index m.

Together, these experimental strategies quantitatively establish the proposed framework's efficacy for dynamic sensor fusion SLAM in unpredictable and previously unmodeled domains.

Evaluation of Experimental Results

Mapping and Trajectory Performance

The aforementioned evaluation of both quantitative data and qualitative observations demonstrates that the proposed dynamic fusion SLAM framework has outperformed static fusion or single-modality approaches in terms of mapping accuracy and trajectory precision. In the controlled indoor assessment environment using ground-truth motion capture, as illustrated in Figure 3, the system has consistently shown a lower cumulative trajectory error than conventional methods, particularly for complex loop-closure paths with repeating elements and transient occlusions [26]. Add real-time sensor reliability adaptation to keep the algorithm from losing accurate global registration in the face of sudden feature loss or light changes that quickly impair vision-or-inertial-only solutions.

An example indoor mission's trajectory overlay is shown in Figure 3(a). The ground-truth path is compared with trajectories from single-sensor, static fusion, and dynamic fusion configurations. In regions with significant lighting gradients, Dynamic Fusion only slightly deviates from the reference and minimises lateral drift. The variation in root-mean-square error with distance travelled is depicted in Figure 3(b). By modifying the trust mechanism, dynamic fusion keeps error persistence within a sub-decimeter envelope when single-modality solutions build drift and deviation, especially when dealing with long ambiguous or low-feature portions [27].

Adaptive multi-sensor fusion can also be used in outdoor performance, as illustrated in Figure 3(c). Endpoint displacement and loop-closure failure in static methods are more likely to occur on unstructured terrain with fluctuating light conditions, shifting shadows, and weak geometric features. Globally consistent maps that can be successfully relocalized following sensor dropout or in reaction to abrupt environmental changes have been consistently created by Dynamically Fused Fusion [28].

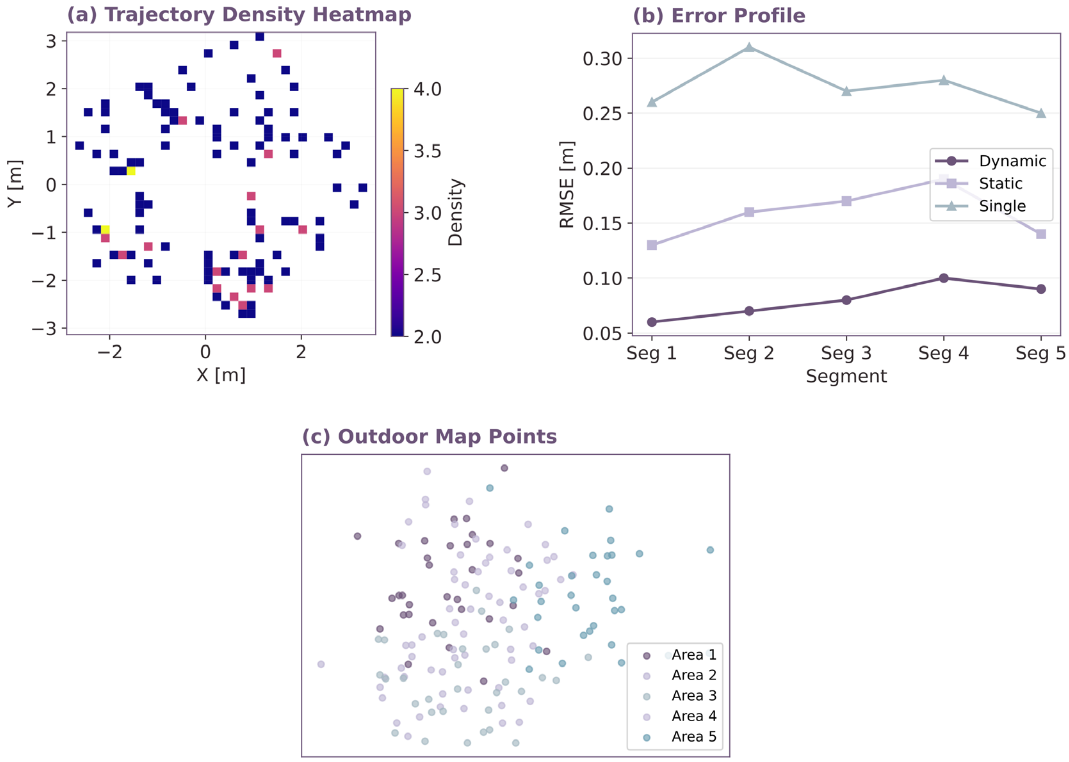

Figure 3. Trajectory Comparison with Dynamic, Static, and Single-Modality Fusion. (a) Trajectory Overlay; (b) Error Profile; (c) Outdoor Mapping.

The variance in mapping and tracking of known and unknown environments across all benchmarks demonstrates that, in the absence of strong prior knowledge or regulated lighting, the adaptive algorithm must evolve autonomously based on sensor influences and maintain a high-precision map [29]. This demonstrates the method's viability in real-world applications in dynamic and unmapped areas [30].

Robustness and Failure Analysis

Introduce a number of targeted disruptions, such as sensor dropouts, abrupt changes in the environment, and quick platform movements, to systematically test the resilience of the suggested dynamic sensor fusion SLAM system. When at least one sensor mode experienced sporadic failure or dynamic interference, the adaptive fusion algorithm outperformed the baseline static and single-sensor configurations in every trial, maintaining trajectory continuity and map consistency.

Three typical disturbance scenarios that have been thoroughly examined based on failures are displayed in Figure 4. The localisation success rate during simulated sensor outages is displayed in Figure 4(a): The dynamic method maintains a continuous real-time tracking rate of over 90% and quickly recovers following sensor restoration, whereas static fusion drastically decreases upon loss of vision or LiDAR. The trajectory divergence index in the case of a high-density moving item or an abrupt shift in light is shown in Figure 4(b). Dynamic fusion may correct these anomalies and re-align to the global map within a minor displacement, whereas the static and single-sensor approaches have substantial estimation leaps or transitory mapping collapse [31]. The time-to-reconvergence following sensor recovery is compared in Figure 4(c); even after a prolonged period without sensors, the adaptive technique typically shows faster relocalization and is frequently within tens of frames.

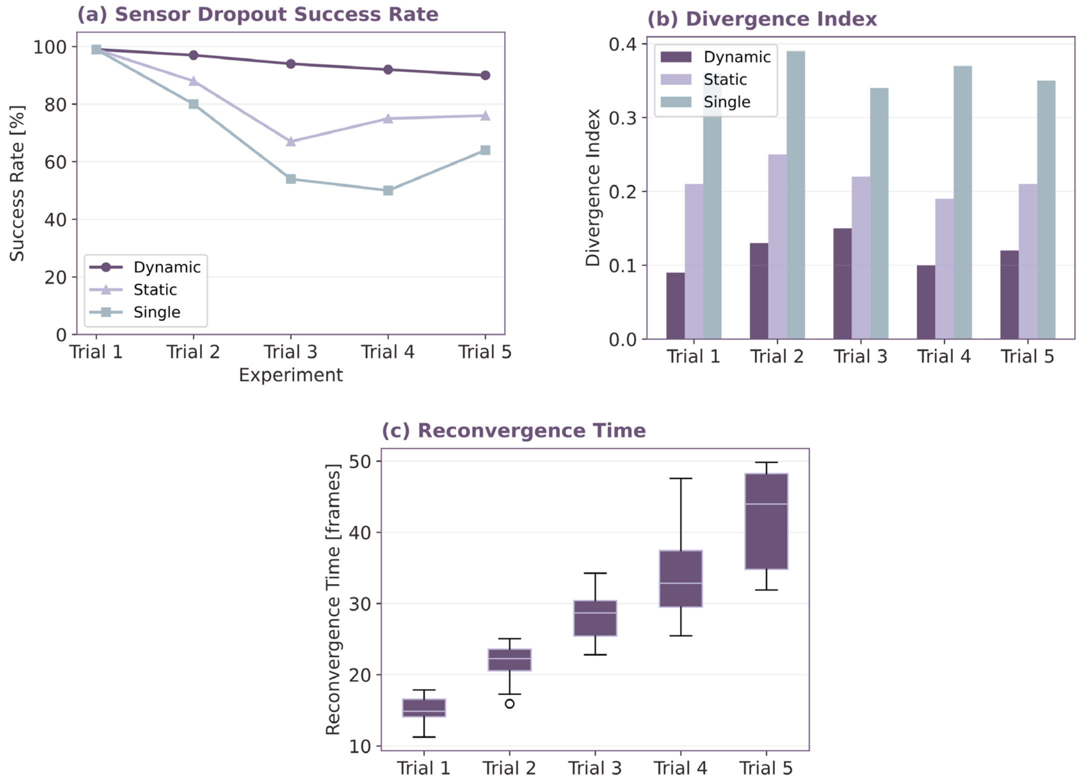

Figure 4. Robustness and Recovery with Dynamic Fusion: (a) Sensor Dropout Success Rate; (b) Divergence Index; (c) Reconvergence Time.

To further evaluate robustness, Figure 5 displays the distribution of errors under adversarial and stochastic disturbances. The distribution of posture estimate errors over a sequence of occlusions is as follows, as illustrated in Figure 5(a): the dynamic fusion system stays relatively near to the mean, while the variance of errors in the static and mono-sensor systems increases dramatically. For inertial-only or visually-weighted approaches, correlated noise in the IMU channel typically causes rapid drift, as seen in Figure 5(b). At this point, dynamically fuse the sensor data to restrict errors to a tolerable range for the mission and avoid major divergence in the system state [32]. The resistance to prolonged visual degradation, such as several consecutive image dropouts, is seen in Figure 5(c); dynamic fusion leverages LiDAR and inertial data to keep tracking when other approaches totally lose localisation.

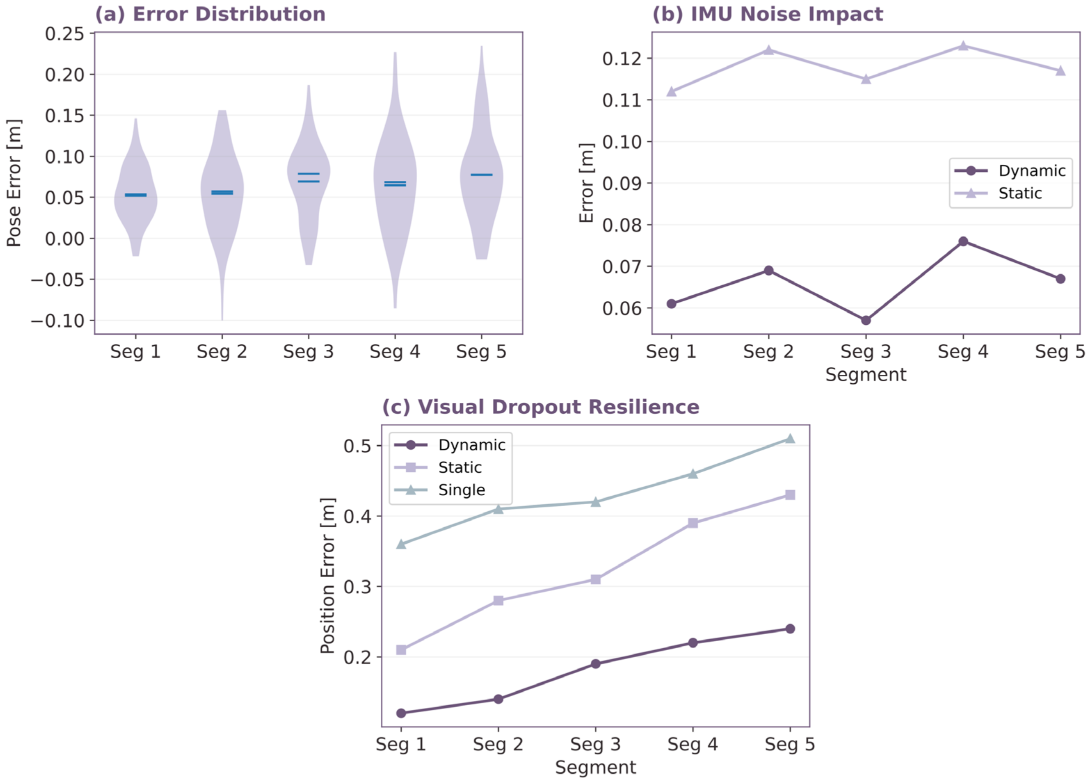

Figure 5. Error Distributions under Disturbance: (a) Occlusion Cycles; (b) IMU Noise Impact; (c) Visual Dropout Resilience.

The aforementioned research indicates that the adaptive fusion approach can still function reasonably well in hostile situations while somewhat enhancing the system's fault tolerance in the event of transient sensor failures [33]. In actual life, the first one will also be used in an unclear or safety-sensitive location, where standard SLAM is likely to perform poorly.

Efficiency and Component Ablation

For real-time, mission-critical robots, strictly minimise computing overhead to satisfy the need for high-performance operation in dynamic fusion SLAM. The system can nevertheless provide timely feedback for autonomous control in all experimental scenarios, with an average end-to-end processing delay of less than 40 ms. The overall calculation performance of the primary fusion modes is displayed in Figure 6. The CPU and GPU utilisation during normal operation and stress tests is depicted in Figure 6(a). While the addition of dynamic sensor reliability estimation is comparatively minor when compared to static fusion, the total resource usage has not reached the saturation limit. Embedded devices with limited resources might benefit from a tiny margin, which must always maintain high efficiency [34].

The dynamic fusion system can maintain peak-rate data processing under a heavy-load condition by choosing the most dependable sensor stream because, as Figure 6(b) illustrates, the frame throughput is still reasonably high when the platform speed and data volume are significant. The distribution of processing latency under full sensor input density and partial sensor dropouts in the system is depicted in Figure 6(c). In the event of brief environmental or sensory disruptions, distribute processing resources adaptively to prevent backlogs and maintain a sub-critical latency in every situation.

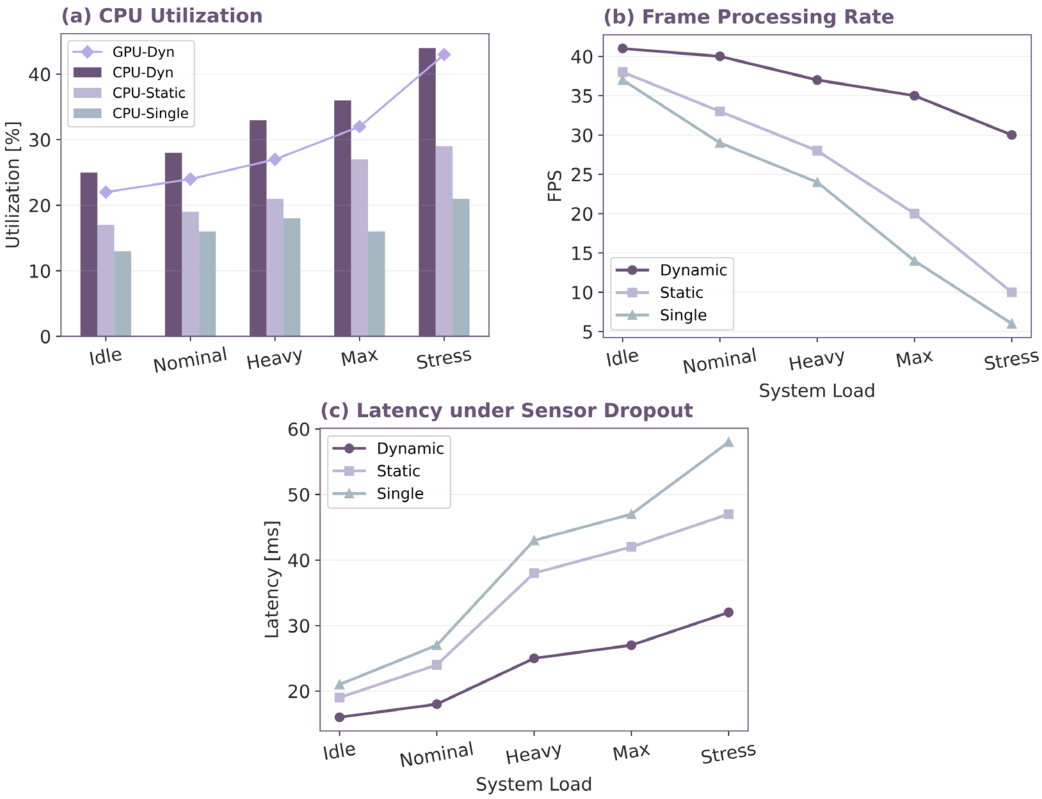

Figure 6. Computational Efficiency and Latency for Dynamic Fusion SLAM: (a) CPU/GPU Utilization; (b) Frame Processing Rate; (c) Latency under Sensor Dropout.

To ascertain the specific contributions of these system modules and sensor inputs to the overall performance, ablation experiments of the components were conducted. The result of methodically eliminating the essential algorithm is depicted in Figure 7. The root-mean-square trajectory error following the individual suppression of the vision, IMU, or LiDAR streams is shown in Figure 7(a); it demonstrates how fragile vision loss is in sparse-feature situations and how severe LiDAR absence is in geometrically confusing or open regions. The duration to relocalization following sensor loss simulation is depicted in Figure 7(b); only dynamic fusion with all adaptation mechanisms activated can accomplish quick and stable state recovery. The mission success rate at various phases of progressive system degradation is depicted in Figure 7(c), and full dynamic fusion performs noticeably better than others under difficult multi-sensor situations [35].

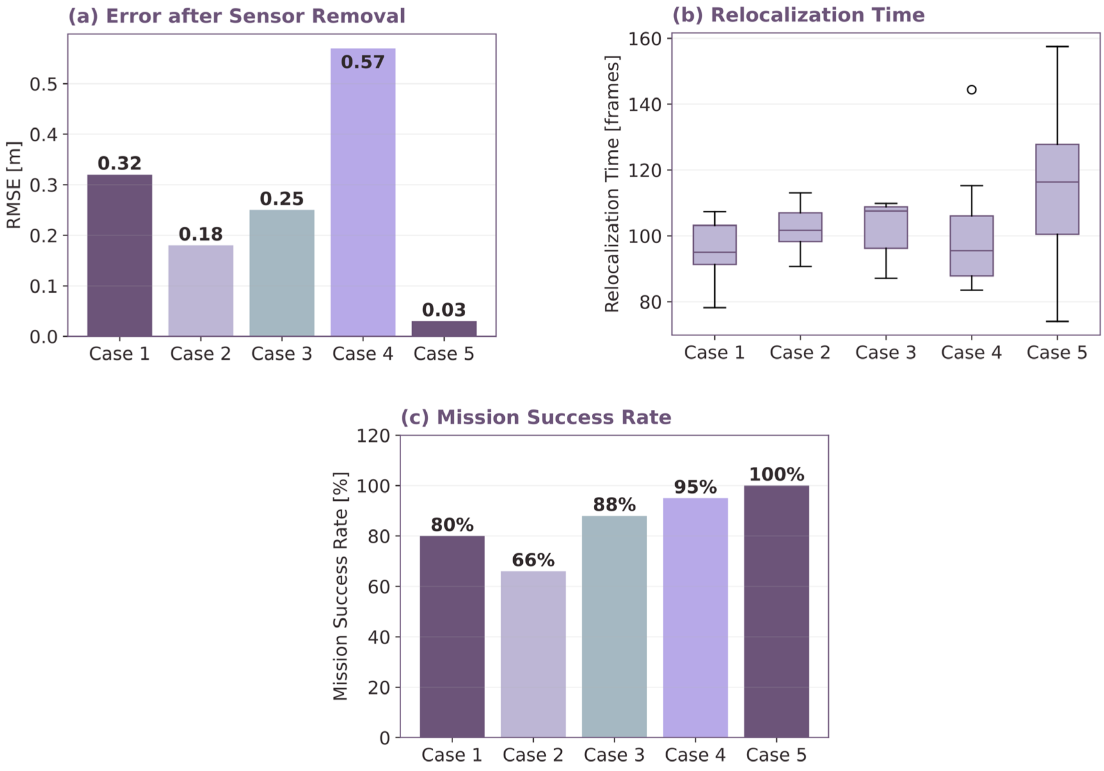

Figure 7. Ablation Effects on SLAM Performance: (a) Error with Sensor Removal; (b) Relocalization Time; (c) Mission Success Rate.

The two systems will cooperate to sustain steady and high-performance functioning in the challenging and unpredictable outdoor environment, according to the aforementioned analysis. The dynamic fusion system's fault-tolerant and highly efficient design has raised the bar for dependable computing performance in multi-sensor SLAM.

Conclusion

The adaptive sensor-fusion SLAM architecture presented in this paper greatly increases the resilience of mapping and localisation in environments lacking a priori maps. The suggested system exhibits strong robustness to transient faults, environmental changes, and modality-specific failures by dynamically modifying the contribution of each sensor stream based on the real-time trust evaluation. To provide continuous, high-accuracy state estimation in bad weather, vision, an inertial measurement unit (IMU), and LiDAR data are tightly integrated, adaptively weighted, and outliers eliminated. The experiments were conducted in a number of challenging indoor and outdoor settings, and it was discovered that the adaptive fusion approach generally outperforms both the static fusion and single-modality baseline approaches in terms of lowering trajectory errors and enhancing loop-closure performance. Ablation investigations have also demonstrated the need for adaptive components; without them, autonomous driving would not be able to recover quickly and maintain map consistency following a sensor failure.

An structured approach for context-aware sensor fusion in SLAM has been made possible by the fusion model. By using data-driven adaptation and quantifying and reacting to real-time signal confidence, this framework overcomes the constraints of rigid, pre-configured fusion techniques, resulting in the realisation of a fully autonomous and self-tuning navigation system. In actuality, the platform's computing efficiency and adaptability may be utilised to create embedded robotic gear, making it possible for long-term environmental observation systems, mobile robots, and autonomous cars. It is appropriate for many real-world applications that are not guaranteed to have acceptable surroundings and sensors since it has demonstrated the ability to adapt to various situations and handle signal loss or other issues in inclement weather.

Nevertheless, certain essential avenues for further research are absent. The existing system is stable, but it hasn't yet employed peer-to-peer collaboration or high-level semantic reasoning to speed up and stabilise large-scale construction site mapping. Long-term, more integrated learning-based identification and distributed SLAM techniques will be needed due to calibration changes, mechanical degradation, or ongoing low-quality observations. To create scalable, cross-domain, and all-weather autonomous systems, keep shrinking algorithms for devices with limited resources and expand empirical validation in real-world, long-term operating conditions.

Author Contributions

Olaf Tadeusz Truskolaski contributes to conceptualization, methodology, software, validation, analysis, investigation, data collection, draft preparation, manuscript editing, visualization, supervision. Barbara Grabowska and Eugeniusz Stępień contribute to data collection, draft preparation, manuscript editing. All authors have read and agreed with the manuscript before its submission and publication.

Funding

This research received no specific financial support from any funding agency.

Institutional Review Board Statement

Not applicable.

References

[1] Xue, J., Cheng, Z., Li, H., Yang, P., Wei, J., & Chen, C. (2024, July). Sensor Fusion SLAM: An Efficient and Robust SLAM system for Dynamic Environments. In 2024 IEEE 25th China Conference on System Simulation Technology and its Application (CCSSTA) (pp. 358-365). IEEE. https://doi.org/10.1109/CCSSTA62096.2024.10691868

[2] Zhao, X., Wen, C., Prakhya, S. M., Yin, H., Zhou, R., Sun, Y., ... & Wang, Y. (2024). Multimodal features and accurate place recognition with robust optimization for LiDAR–visual–inertial SLAM. IEEE Transactions on Instrumentation and Measurement, 73, 1-16. https://doi.org/10.1109/TIM.2024.3370762

[3] Zhumu, F., Yuxuan, L., Pengju, S., Fazhan, T., & Nan, W. (2023). A multisensor high-precision location method in urban environment. IEEE Systems Journal, 17(4), 6611-6622. https://doi.org/10.1109/JSYST.2023.3316140

[4] Xu, Y., Zheng, R., Zhang, S., Liu, M., & Yu, J. (2024). Uncertainty-aware autonomous robot exploration using confidence-rich localization and mapping. IEEE Transactions on Automation Science and Engineering, 22, 1124-1138. https://doi.org/10.1109/TASE.2024.3360442

[5] Hegde, A. A., & Shetty, S. (2024, December). Visual slam in dynamic environments: Robustness and adaptability. In 2024 Fourth International Conference on Multimedia Processing, Communication & Information Technology (MPCIT) (pp. 78-85). IEEE. https://doi.org/10.1109/MPCIT62449.2024.10892624

[6] Shi, P., Zhu, Z., Sun, S., Rong, Z., Zhao, X., & Tan, M. (2023). Covariance estimation for pose graph optimization in visual-inertial navigation systems. IEEE Transactions on Intelligent Vehicles, 8(6), 3657-3667. https://doi.org/10.1109/TIV.2023.3263837

[7] Rahman, S., DiPietro, R., Kedarisetti, D., & Kulathumani, V. (2024, October). Large-scale indoor mapping with failure detection and recovery in slam. In 2024 IEEE/RSJ International Conference on Intelligent Robots and Systems (IROS) (pp. 12294-12301). IEEE. https://doi.org/10.1109/IROS58592.2024.10802593

[8] Cai, Y., Ou, Y., & Qin, T. (2024). Improving SLAM techniques with integrated multi-sensor fusion for 3D reconstruction. Sensors, 24(7), 2033. https://doi.org/10.3390/s24072033

[9] Lai, T. (2022). A review on visual-slam: Advancements from geometric modelling to learning-based semantic scene understanding using multi-modal sensor fusion. Sensors, 22(19), 7265. https://doi.org/10.3390/s22197265

[10] Wang, C., & Qiu, Y. (2023, November). Electronic Sensor Multi-Modal Slam Algorithm Based on Information Fusion Technology. In 2023 International Conference on Ambient Intelligence, Knowledge Informatics and Industrial Electronics (AIKIIE) (pp. 1-6). IEEE. https://doi.org/10.1109/AIKIIE60097.2023.10390439

[11] Chen, W., Wang, X., Gao, S., Shang, G., Zhou, C., Li, Z., ... & Hu, K. (2023). Overview of multi-robot collaborative SLAM from the perspective of data fusion. Machines, 11(6), 653. https://doi.org/10.3390/machines11060653

[12] Wadoux, A. M. C., Heuvelink, G. B., De Bruin, S., & Brus, D. J. (2021). Spatial cross-validation is not the right way to evaluate map accuracy. Ecological Modelling, 457, 109692. https://doi.org/10.1016/j.ecolmodel.2021.109692

[13] Gupta, A., & Fernando, X. (2022). Simultaneous localization and mapping (slam) and data fusion in unmanned aerial vehicles: Recent advances and challenges. Drones, 6(4), 85. https://doi.org/10.3390/drones6040085

[14] Shen, K., Li, Y., Liu, T., Zuo, J., & Yang, Z. (2023). Adaptive-robust fusion strategy for autonomous navigation in GNSS-challenged environments. IEEE Internet of Things Journal, 11(4), 6817-6832. https://doi.org/10.1109/JIOT.2023.3315758

[15] Merveille, F. F. R., Jia, B., Xu, Z., & Fred, B. (2024). Advancements in sensor fusion for underwater SLAM: A review on enhanced navigation and environmental perception. Sensors, 24(23), 7490. https://doi.org/10.3390/s24237490

[16] Xia, Y., Cheng, J., Cai, X., Zhang, S., Zhu, J., & Zhu, L. (2022). SLAM back-end optimization algorithm based on vision fusion IPS. Sensors, 22(23), 9362. https://doi.org/10.3390/s22239362

[17] Huang, P., Zeng, L., Chen, X., Luo, K., Zhou, Z., & Yu, S. (2022). Edge robotics: Edge-computing-accelerated multirobot simultaneous localization and mapping. IEEE Internet of Things Journal, 9(15), 14087-14102. https://doi.org/10.1109/JIOT.2022.3146461

[18] Nawaz, M., Tang, J. K. T., Bibi, K., Xiao, S., Ho, H. P., & Yuan, W. (2023). Robust cognitive capability in autonomous driving using sensor fusion techniques: A survey. IEEE Transactions on Intelligent Transportation Systems, 25(5), 3228-3243. https://doi.org/10.1109/TITS.2023.3327949

[19] Sun, G., Zhang, Z., Zheng, B., & Li, Y. (2019). Multi-sensor data fusion algorithm based on trust degree and improved genetics. Sensors, 19(9), 2139. https://doi.org/10.3390/s19092139

[20] Cheng, J., Zhang, L., Chen, Q., Fu, Z., & Du, L. (2024). High precision and robust vehicle localization algorithm with visual-LiDAR-IMU fusion. IEEE Transactions on Vehicular Technology, 73(8), 11029-11043. https://doi.org/10.1109/TVT.2024.3379435

[21] Zhang, J., Yuan, L., Ran, T., Tao, Q., & Wu, Z. (2023). Outlier elimination for monocular object SLAM based on spatiotemporal consistency constraints. IEEE Sensors Journal, 23(8), 8887-8898. https://doi.org/10.1109/JSEN.2023.3252050

[22] Xiang, X., Li, K., Huang, B., & Cao, Y. (2022). A multi-sensor data-fusion method based on cloud model and improved evidence theory. Sensors, 22(15), 5902. https://doi.org/10.3390/s22155902

[23] Terblanche, J., Claassens, S., & Fourie, D. (2021). Multimodal navigation-affordance matching for slam. IEEE Robotics and Automation Letters, 6(4), 7728-7735. https://doi.org/10.1109/LRA.2021.3098788

[24] Pan, H., Liu, D., Ren, J., Huang, T., & Yang, H. (2024). LiDAR-IMU tightly-coupled SLAM method based on IEKF and loop closure detection. IEEE Journal of Selected Topics in Applied Earth Observations and Remote Sensing, 17, 6986-7001. https://doi.org/10.1109/JSTARS.2024.3357536

[25] Wang, Y., Tian, Y., Chen, J., Xu, K., & Ding, X. (2024). A survey of visual SLAM in dynamic environment: The evolution from geometric to semantic approaches. IEEE Transactions on Instrumentation and Measurement, 73, 1-21. https://doi.org/10.1109/TIM.2024.3420374

[26] Silva, F. A., Brito, C., Araújo, G., Fé, I., Tyan, M., Lee, J. W., ... & Maciel, P. R. M. (2022). Model-driven impact quantification of energy resource redundancy and server rejuvenation on the dependability of medical sensor networks in smart hospitals. Sensors, 22(4), 1595. https://doi.org/10.3390/s22041595

[27] Chen, W., Zhu, L., He, L., Guan, Y., & Zhang, H. (2019). Reliable visual exploration system with fault tolerance structure. Applied Sciences, 9(4), 662. https://doi.org/10.3390/app9040662

[28] Macktoobian, M., Shu, Z., & Zhao, Q. (2023). Topology recoverability prediction for ad-hoc robot networks: A data-driven fault-tolerant approach. IEEE Transactions on Signal and Information Processing over Networks, 9, 786-799. https://doi.org/10.1109/TSIPN.2023.3328275

[29] Guo, J., Wang, S., Mao, Y., Wang, G., Wu, G., Wu, Y., & Liu, Z. (2024). Supervised learning study on ground classification and state recognition of agricultural robots based on multi-source vibration data fusion. Computers and Electronics in Agriculture, 219, 108791. https://doi.org/10.1016/j.compag.2024.108791

[30] Chiang, K. W., Le, D. T., Duong, T. T., & Sun, R. (2020). The performance analysis of INS/GNSS/V-SLAM integration scheme using smartphone sensors for land vehicle navigation applications in GNSS-challenging environments. Remote Sensing, 12(11), 1732. https://doi.org/10.3390/rs12111732

[31] Wang, T., Su, Y., Shao, S., Yao, C., & Wang, Z. (2021, September). Gr-fusion: Multi-sensor fusion slam for ground robots with high robustness and low drift. In 2021 IEEE/RSJ International Conference on Intelligent Robots and Systems (IROS) (pp. 5440-5447). IEEE. https://doi.org/10.1109/IROS51168.2021.9636232

[32] Khedekar, N., Kulkarni, M., & Alexis, K. (2022, October). Mimosa: A multi-modal slam framework for resilient autonomy against sensor degradation. In 2022 IEEE/RSJ International Conference on Intelligent Robots and Systems (IROS) (pp. 7153-7159). IEEE. https://doi.org/10.1109/IROS47612.2022.9981108

[33] Kazeminasab, S., Sadeghi, N., Janfaza, V., Razavi, M., Ziyadidegan, S., & Banks, M. K. (2021). Localization, mapping, navigation, and inspection methods in in-pipe robots: A review. IEEE access, 9, 162035-162058. https://doi.org/10.1109/ACCESS.2021.3130233

[34] Chen, L., Li, G., Xie, W., Tan, J., Li, Y., Pu, J., ... & Shi, W. (2024). A survey of computer vision detection, visual SLAM algorithms, and their applications in Energy-Efficient autonomous systems. Energies, 17(20), 5177. https://doi.org/10.3390/en17205177

[35] Lv, X., He, Z., Yang, Y., Nie, J., Dong, Z., Wang, S., & Gao, M. (2024). MSF-SLAM: Multi-sensor-fusion-based simultaneous localization and mapping for complex dynamic environments. IEEE Transactions on Intelligent Transportation Systems, 25(12), 19699-19713. https://doi.org/10.1109/TITS.2024.3451996